Opto-Electronics Review 29 (2021) 91-96

PAN POLISH ACADEMY OF SCIENCES

Opto-Electronics Review

journal homepage: http://journals.pan.pl/opelre

Signal processing for time resolved photoluminescence spectroscopy

K. Grodecki*, K. Murawski, J. Rutkowski, A. Kowalewski, J. Sobieski

Military University of Technology, 2 Kaliskiego St., Warsaw 00-908, Poland

Article info

Article history:
Received 25 Jun. 2021
Received in revised form 4 Aug. 2021
Accepted 05 Aug. 2021

Keywords:
epitaxy, HgCdTe, photoluminescence, time resolved photoluminescence

Abstract

Accurate determination of material parameters, such as carrier lifetimes and defect activation energy, is a significant problem in the technology of infrared detectors. Among many different techniques, using the time resolved photoluminescence spectroscopy allows to determine the narrow energy gap materials, as well as their time dynamics. In this technique, it is possible to observe time dynamics of all processes in the measured sample as in a streak camera. In this article, the signal processing for the above technique for $Hg_{1-x}Cd_xTe$ with a composition x of about 0.3 which plays an extremely important role in the mid-infrared is presented.

Machine learning algorithms based on the independent components analysis were used to determine components of the analyzed data series. Two different filtering techniques were investigated. In the article, it is shown how to reduce noise using the independent components analysis and what are the advantages, as well as disadvantages, of selected methods of the independent components analysis filtering. The proposed method might allow to distinguish, based on the analysis of photoluminescence spectra, the location of typical defect levels in HgCdTe described in the literature.

1. Introduction

HgCdTe-based devices are still heavily used to detect infrared radiation. Due to the dependence of the energy gap on the chemical composition, devices based on this technology can operate in a wide range of radiation [1–3]. The $Hg_{1-x}Cd_xTe$ material with the moll fraction $x \leq 0.3$ still plays an extremely important role in the production of mid-infrared detectors [1,4–8]. In this paper, the experimental results of time resolved photoluminescence spectroscopy (TRPLS) for the detection layer with HgCdTe optimized at 3.4 μm for 230 K are presented. Similar structures have already been described in the literature [9–11]. In spectrum of photoluminescence (PL), there are not only transitions from the energy gap, but also peaks related to impurities associated with defect-related transitions [9–11].

Accurate determination of carrier lifetimes is a key factor in determining basic photodetector parameters, such as response time and detectivity, as well as material parameters, such as defect levels of activation energy.

TRPLS experiments are difficult to perform due to the lack of lock-in and, thus, no reinforcement. By using machine learning (ML) algorithm based on independent components analysis (ICA), the measured signal can be enhanced [12]. This method was already used to extract Si-H bonds in the Raman spectra of the hydrogen intercalated graphene [13]. In our experiment, in TRPLS a matrix consisting of the measured IR spectrum on one axis and time on the second axis was obtained. The idea of ICA filtering means that for some series of spectra (or more generally - parameters), the set of spectra that are independent and may build any of the source spectrum is wanted. For example, while measuring a sample with three different materials in ICA, the spectrum of each material in each input spectrum can be extracted. Finally, each spectrum using the components which have been found can be rebuilt. Using this method, noise can be reduced more than 200 times.

*Corresponding author at: kacper.grodecki@wat.edu.pl

https://doi.org/10.24425/opelre.2021.139038.
1896-3757/ Association of Polish Electrical Engineers (SEP) and Polish Academic of Sciences (PAS). Published by PAS

2. Experimental details

To perform TRPLS, there were used: an optical parametrical oscillator (OPO) as the excitation source, a Bruker Vertex 70 V FT-IT spectrometer with an MCT Vigo photodetector thermoelectrically cooled, optimized at 10.6 μm, detectivity D* of 1×10^{10} cmHz^{½}/W, and the response time of 1 ns, to collect the PL signal. A Keyseight 4-GHz oscilloscope was used to analyze the signal from the photodetector. The sample was in a helium cryostat. Details of the experimental TRPLS creation system were covered in our previous article [14]. Here, we upgraded the system by using a vacuum chamber for the photodetector, so that the entire PL path was under vacuum. As the excitation wavelength, a 2400-nm filter was used to remove the laser signal. All measurements were made in a vacuum at a temperature of 100 K. In the experiment, a spectral resolution of 3 cm^{-1} was performed, in order to be able to distinguish all peaks that were detected by other groups. Time-resolution was estimated at 2 ns because of the photodetector limitation.

Usually, to perform TRPLS, a gray filter is used to obtain a low excitation regime and, therefore, to measure the minority carrier decay. In the described experiment, no filter was used because the PL signal was too low, so it was not in the low excitation regime.

$Hg_{0.695}Cd_{0.305}Te$ (MCT) sample was manufactured in a joint laboratory run by VIGO System and the Military University of Technology in Warsaw, Poland. The heterostructure was grown on 2" semi-insulating 2 degree-oriented GaAs (100) substrates in a horizontal MOCVD AIX 200 reactor. Inter-diffused multilayer process (IMP) technique was applied to deposit the HgCdTe layer. A detailed description of the implemented MOCVD growth procedure is presented in Ref. 3. Sample was initially undoped with an acceptor concentration of 3×10^{-15} cm^{-3} at room temperature and a Cd mole fraction was of 0.305. The thickness of the layer was of 4 μm.

To perform ICA filtering, over 200 experimental points are needed. In the IR spectrum, the number of points depends on the resolution and the spectrum length. In the experiment, there is over 4000 points. The number of points on the timeline depends on the oscilloscope sampling and the time length. In the study, a 40-Gsa/s sampling and a 500-ns length were used. Due to the difference between the photodetector and the oscilloscope resolution, every 20 points were also averaged. Finally, $500 \times 40/20 = 1000$ points on the timeline were obtained. For each axis, more than 1000 points were obtained which is enough to perform ICA filtering.

2.1. ICA filtering technique

In our system, the ICA filtering can be performed in two different directions which will be called in the article: "time method" and "spectral method". In the time method filtering, the spectrum is treated as a series of points and the entire map as a series of decaying signals, which means we were looking for 15 similar decaying signals that constructed our 4000 signals across the map. In the spectral method, each decaying signal is treated as a series of points and the whole map as a series of spectra.

For each method the procedure is the same and the basic matrix comes from the same data. However, in the time method, the matrix is transposed with respect to the spectral method. Thus, the "input data" are the same, but the matrices built are not the same.

The idea of ICA is to figure out independent components of the measured signal, i.e., if the signal is a human voice [15,16], the problem is how to separate voices from people talking simultaneously in one room: the problem known as the cocktail party problem. There are two people generating two voices S1 and S2 and there are two microphones X1 and X2. As described in Ref. 15, mixed signals detected by microphones X1 and X2 could be expressed as:

$$X(t) = A \times S(t) + v(t), \tag{1}$$

where A is the unknown mixing matrix, $S(t)$ are the source signals, $X(t)$ are the measured signals, and $v(t)$ are the additive noises. In the spectral method, it can be assumed that $S(t)$ are the initial transitions or peaks inside PL spectrum, $X(t)$ are the measured spectra, and $v(t)$ is the noise. The solution is to find the matrix W which transforms the signal $X(t)$ to get the estimation of the $S(t)$:

$$\hat{S}(t) = W \times X(t). \tag{2}$$

On the other hand, after Eq. (1):

$$\hat{S}(t) = A \times S(t) + v(t), \tag{3}$$

where, $\hat{S}(t)$ is the estimation of $S(t)$. Usually, neither A nor W are known, so $S(t)$ cannot be directly calculated, however, it can be estimated. A very important assumption is that $S(t)$ must be statistically independent and do not have a Gaussian distribution.

To solve this problem, the ICA fast algorithm was used. The first step is to find the linear U transform that makes the signal $X(t)$ uncorrelated, and the unit-variance is called whitening.

$$\hat{X}(t) = U \times X(t) \tag{4}$$

what changes the equation to:

$$\hat{S}(t) = W \times \hat{X}(t). \tag{5}$$

To calculate W, kurthosis can be used which is defined as:

$$kurt(S_i) = E[S_i^4] - 3(E[S_i^2])^2 \tag{6}$$

where i is the number of source signals in the vector S.

The cost function is as follows:

$$kurt\left(w^T \hat{X}_\iota\right) = E\left[\left(w^T \hat{X}_\iota{}^4\right)\right] - 3\left(E\left[\left(w^T \hat{X}_\iota{}^4\right)^2\right]\right)^2. \tag{7}$$

When using the fix-point algorithm, the iteration is:

$$w_i(k) = E\left[\hat{X}_\iota\left(w_i(k-1)^T \hat{X}_\iota\right)^3\right] - 3w_i(k-1). \tag{8}$$

Then, the procedure may be described as follows:

1. Make the signal mean zero;
2. Whiten the signal;
3. Make $i = 1$;
4. Choose the initial W and $k = 1$;
5. Make $w_i(k)$ as in Eq. (7);
6. Normalize $w_i(k)$;
7. If the increase of $k = k + 1$, go to Eq. (4);
8. Make $i = I + 1$;
9. When $i <$ number of origin signals, go back to Eq. (4). The process is iterated until the weight $w_i(k)^T w_i(k-1)$ is equal or close to 1.

Given W, the origin signal S can be calculated with Eq. (4). The entire procedure can be performed using Python and the scikit-learn library.

Remember that in the spectrum measured by FT-IR the interferogram is measured and it is apodized to calculate the spectrum. Only points close to the center of the interferogram have the greatest influence. On the other hand, in the decaying signal only points close to the beginning of the zero time, plus the duration of the longest process, have non-zero intensity. That means that only 20–30% of the points on our map are not noise. These 20-30% of the points mean that one should be careful when using the ICA algorithm.

Spectra figures [Fig. 1(c), Fig. 2, Fig. 3, and Fig. 5(b)-(d)] are on a linear scale while the signal decay (Fig. 4 and Fig. 6) is on a logarithmic scale. TRPLS maps [Fig. 1(a)-(b) and Fig. 5(a)] are on a linear scale of energy (x-axis) and time (y-axis) while intensity (color scale) is on a logarithmic scale.

3. Results and discussion

3.1. *Part 1 – time method*

In Fig. 1, TRPLS maps for unfiltered map (a) and time method filtered map (b) are presented. The enhanced signal has a much lower background level (navy blue close to 0.01 with respect to green close to 0.1) which means a much better signal-to-noise ratio. In the pure signal, there are also visible many oscillations that look like “braids” and many of them seem to be separate time-resolved spectral peaks. In Fig. 1(c), a closer look at these “braids” (in black rectangles) clearly shows that these are some unknown fluctuations, first, because the existence of separate peaks of full width at half maximum (FWHM) below 1–2 meV is impossible, second, they are repetitive for different time. These fluctuations may be due to the oscilloscope signal. In the filtered image, the same effect is suppressed. However, there can also be some vertical and horizontal lines which also should not exist in a well-performed map, and they may signify some fluctuations performed by the equipment or ICA filtering.

A closer look at the separated spectra gives more information on what is enhanced and what is distorted using the presented method.In Fig. 2, pure spectra and enhanced spectra for the times 0 (a), 50 (b), and 100 ns (c)

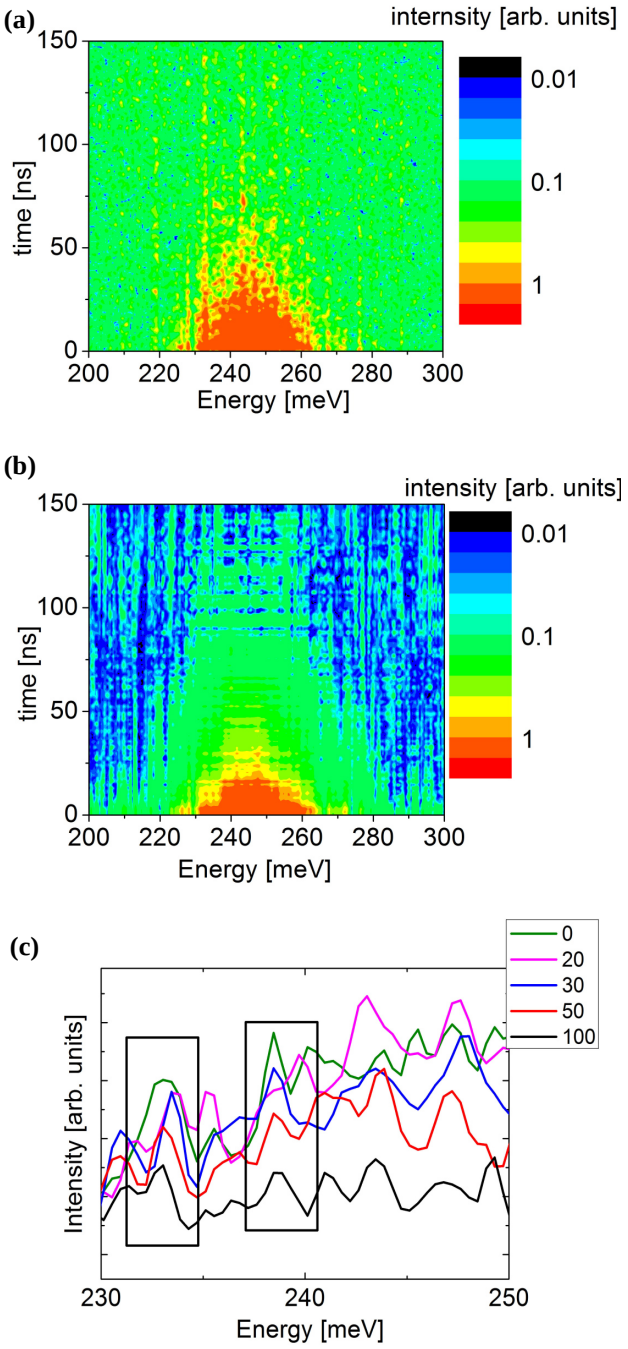

Fig. 1. TRPLS map for pure signal (a), signal enhanced by the time method (b), and a closer look at the pure spectra to emphasize fluctuations (black rectangles) (c).

after laser excitation are presented. For each spectrum, the signal-to-noise ratio is much better for the enhanced one, however, the signal dynamics is the same.

In Fig. 3, a summary of the pure signal without [Fig. 3(a)] and with [Fig. 3(b)] the time method application is presented. In Fig. 3(b), not only a much higher signal-to-noise ratio can be seen, but, also, several peaks which cannot be separated in Fig. 3(a) can be distinguished. Also, there can be distinguished 5 strong peaks [based on multi-gaussian fitting presented in Fig. 3(b)] 226, 233, 240, 250, and 271 meV (marked as blue lines). Most of them are

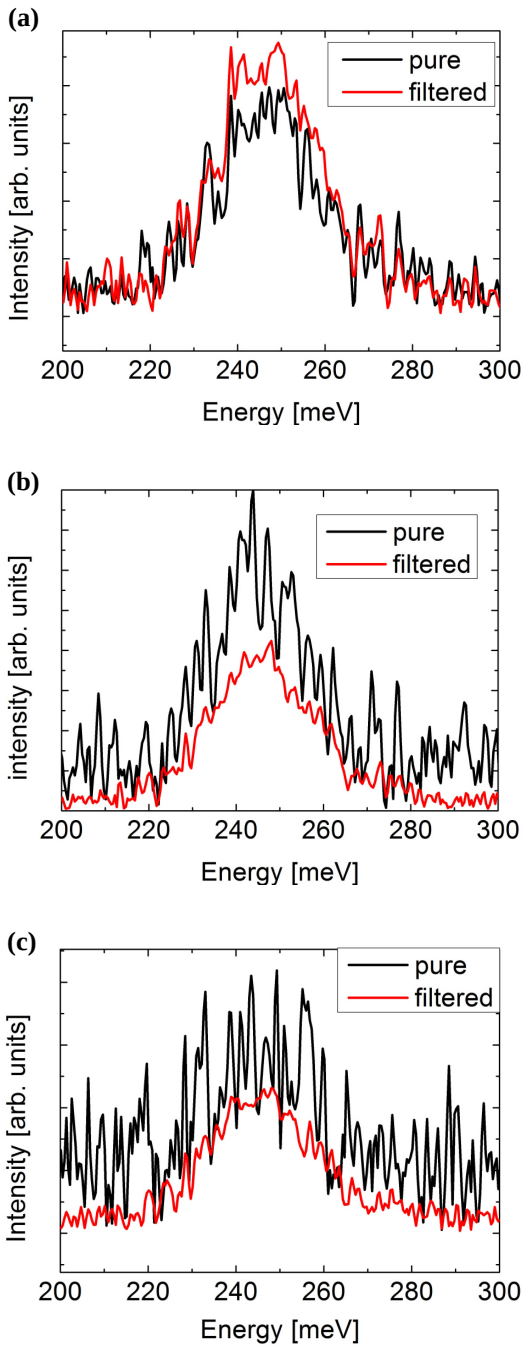

Fig. 2. PL signal for pure signal (black) and with the ICA time method (red) for 0 ns (a), 50 ns (b), 100 ns (c) after laser excitation.

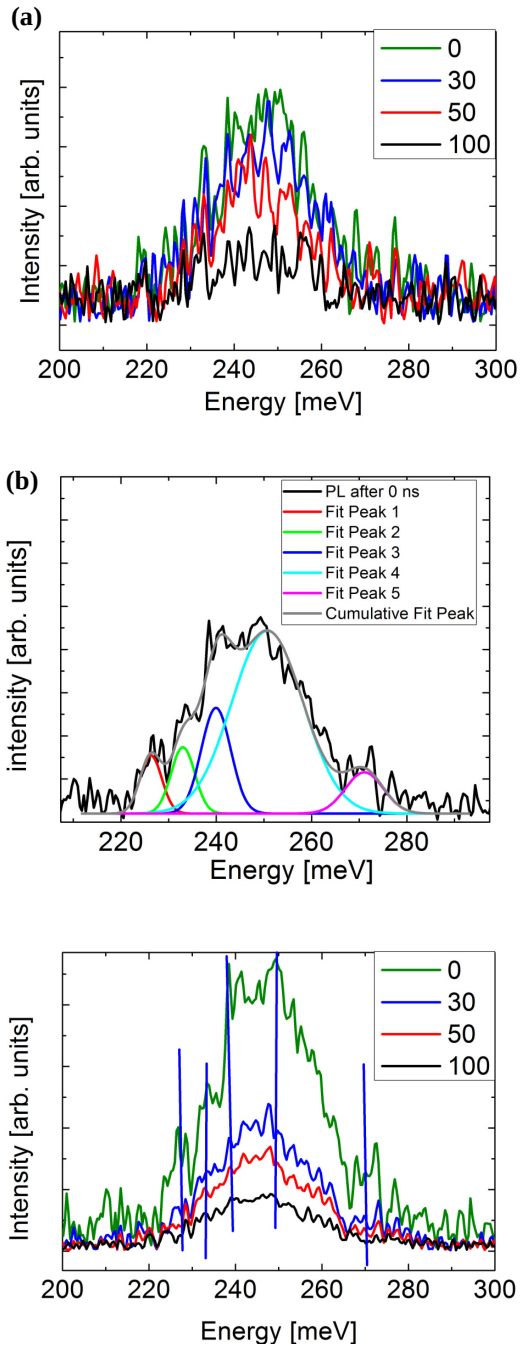

Fig. 3. Composition of spectra performed at 0, 30, 50 and 100 ns after laser stop for pure signal (a), multi-gaussian fitting for 0 ns after laser showing existence of 5 peaks (b), and signal filtered using time method (c).

close to those described in the literature 250, 240, 230, 225 meV [17,18]. It is not obvious whether the peak at 270 meV is a signal or some fluctuation, however, in Ref. 11, the similar uncommented structure at higher energy (about 290 meV) can be found.

The second piece of information that may be found on the TRPLS map is the lifetime. In this case, only majority carriers can be measured because the excitation energy is too high. Comparison of a decaying signal for the highest peak (250 meV) is presented in Fig. 4. It can be seen, that both lines do not have the same decay dynamics and, thus, decay time. Also, the filtered decay is not strongly enhanced in comparison to the pure signal. Analyzing this Figure, it can be observed that visible noise or fluctuations

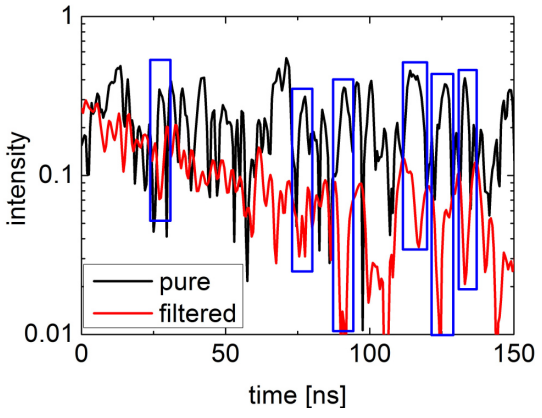

Fig. 4. Comparison of the PL signal for the method with (red) and without (black) filtered time.

(denoted by blue rectangles) in the filtered signal are in the same place in time, as in the original signal which indicates that they are getting stronger or, at least, not extinguishing.

Summarizing this section, it can be concluded that by using the time method, the PL spectra can be enhanced. However, the PL decay signal is modified with the time method which means that filtering by this method should not be performed to determine the PL decay. As it was mentioned, by enhancing the signal, repeatable fluctuations are also enhanced. Probably there are many fluctuations in the decaying signal (it is the signal from the oscilloscope), so these fluctuations strongly disturb the real signal.

3.2. *Part 2 – spectral method*

As mentioned before, filtering can be applied in a direction different than in the time method. Figure 5 shows: map (a) and spectra (b)–(d) for the application of the spectral method. In Fig. 5(a), for 0 ns almost no difference can be seen between the pure and the enhanced signal, however, for 100 ns [Fig. 5(b)] the signal-to-noise ratio is higher for the filtered signal than for the pure one.

Unfortunately, many oscillations were also enhanced which can be better observed in Fig. 5(c) (marked as blue rectangles). Most of "high noise" that can be found in Fig. 5(b) can be treated as enhanced fluctuations because they are repeatable for different times [Fig. 5(c)]. It means that by performing the spectral method, the signal can be enhanced, as well as the fluctuations. The same situation was already seen for the time method.

Figure 6 shows the decaying signal for the main peak presented in Fig. 3(b). The filtered signal has a much higher signal-to-noise ratio than the pure one, and the dynamics of the red and the black curve are the same. Moreover, it is possible to estimate the red curve lifetime, whereas for the black one it is impossible.

The estimated lifetime (about 700 ns) is shorter than it should be for the HgCdTe samples (around 4 μs). There are two main reasons for this. The first one is that the studying of the sample took a long time, so the sample was modified in such a way that only the surface states could be seen. The surface effects have shorter lifetimes than the bulk material. The second reason can be the use of a quite high laser energy, thus we measure majority carriers, not minority, which makes the lifetime shorter.

4. Conclusions

In this article, it is presented how to apply ICA filtering to TRPLS measurements. It was shown that by treating the matrix as a series of spectra, a PL decay signal can be enhanced, and by treating the data as a series of decays, the spectra can get filtered. The ICA filtering boosts not only signal but also fluctuations, however, fluctuations are enhanced only in the filtered series, not in the perpendicular one. That means that the spectra should be analyzed using the time filtering method and the signal decays should be analyzed using the spectral filtering method.

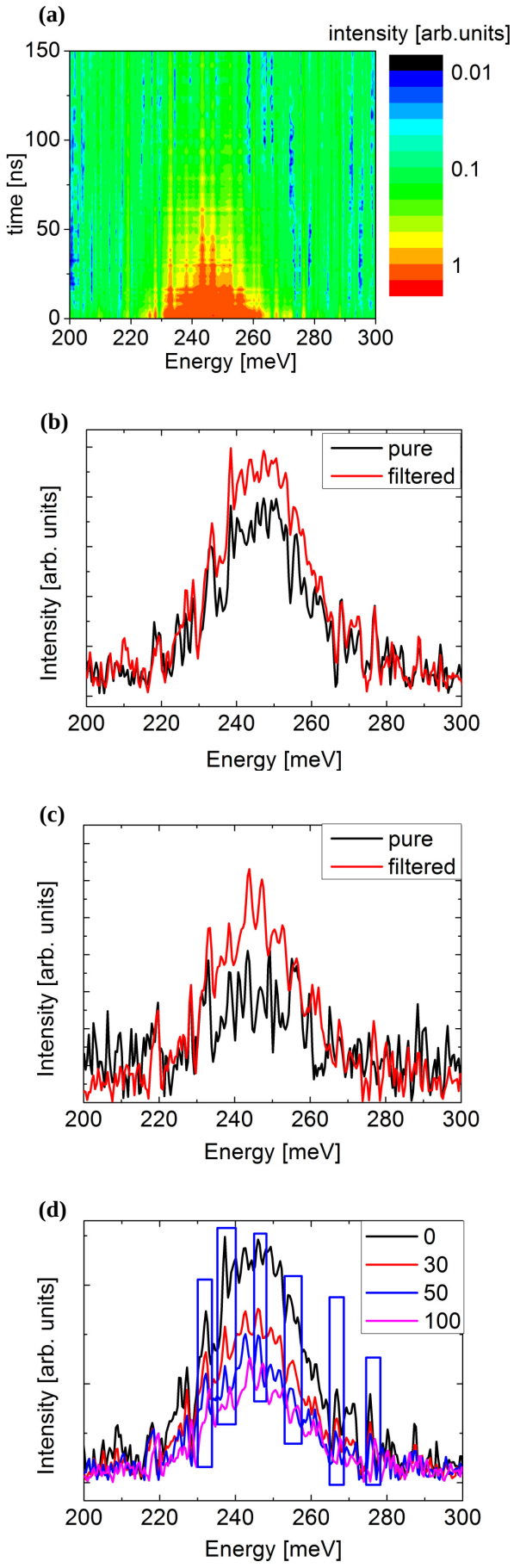

Fig. 5. TRLPS map for spectral filtering (a). PL signal for without (black) and with ICA spectral method (red) for 0 ns after laser stop (b), 100 ns after stop (c), and composition of spectra (d).

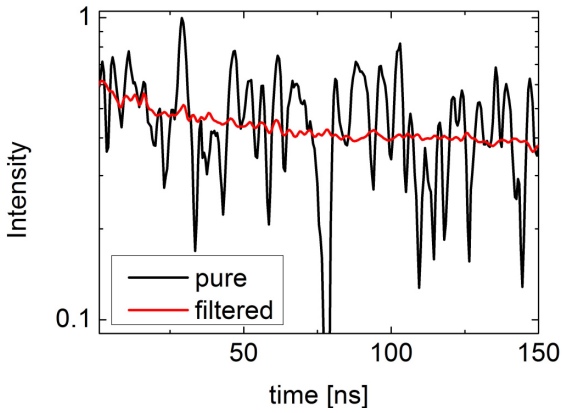

Fig. 6. Comparison of PL decay without (black) and with the spectral method (red).

Acknowledgements

The paper was partially supported by the National Science Centre (Poland), grant no. UMO-2019/33/B/ST7/00614 and National Science Centre (Poland), grant no. 2017/27/B/ST7/01507.

References

[1] Kopytko, M. *et al.* High-operating temperature MWIR nBn HgCdTe detector grown by MOCVD. *Opto-Electron. Rev.* **21**, 402–405 (2013). https://doi.org/10.2478/s11772-013-0101-y

[2] Kopytko, M., Kebłowski, A., Gawron, W. & Madejczyk, P. Different cap-barrier design for MOCVD grown HOT HgCdTe barrier detectors. *Opto-Electron. Rev.* **23**, 143–148 (2015). https://doi.org/10.1515/oere-2015-0017

[3] Rogalski, A. HgCdTe infrared detector material: History, status and outlook. *Rep. Prog. Phys.* **68**, 2267–2336 (2005). https://doi.org/10.1088/0034-4885/68/10/R01

[4] Bhan, R. K. & Dhar, V. Recent infrared detector technologies, applications, trends and development of HgCdTe based cooled infrared focal plane arrays and their characterization. *Opto-Electron. Rev.* **27**, 174–193 (2019). https://doi.org/10.1016/j.opelre.2019.04.004

[5] Izhnin, I. *et al.* Photoluminescence of HgCdTe nanostructures grown by molecular beam epitaxy on GaAs. *Opto-Electron. Rev.* **21**, 390–394 (2013). https://doi.org/10.2478/s11772-013-0103-9

[6] Madejczyk, P. *et al.* Control of acceptor doping in MOCVD HgCdTe epilayers. *Opto-Electron. Rev.* **18**, 271–276 (2010). https://doi.org/10.2478/s11772-010-1023-x

[7] Martyniuk, P., Koźniewski, A., Kebłowski, A., Gawron, W. & Rogalski, A. MOCVD grown MWIR HgCdTe detectors for high operation temperature conditions. *Opto-Electron. Rev.* **22**, 118–126 (2014). https://doi.org/10.2478/s11772-014-0186-y

[8] Piotrowski, J. *et al.* Uncooled MWIR and LWIR photodetectors in Poland. *Opto-Electron. Rev.* **18**, 318–327 (2010). https://doi.org/10.2478/s11772-010-1022-y

[9] Wang, H., Hong, J., Yue, F., Jing, C. & Chu, J. Optical homogeneity analysis of Hg1−xCdxTe epitaxial layers: How to circumvent the influence of impurity absorption bands? *Infrared Phys. Technol.* **82**, 1–7 (2017). https://doi.org/10.1016/j.infrared.2017.02.007

[10] Yue, F., Wu, J. & Chu, J. Deep/shallow levels in arsenic-doped HgCdTe determined by modulated photoluminescence spectra. *Appl. Phys. Lett.* **93**, 131909 (2008). https://doi.org/10.1063/1.2983655

[11] Yue, F. Y. *et al.* Optical characterization of defects in narrow-gap HgCdTe for infrared detector applications. *Chin. Phys. B* **28**, 17104 (2019). https://doi.org/10.1088/1674-1056/28/1/017104

[12] Hyvärinen, A. & Oja, E. Independent component analysis: Algorithms and applications. *Neural Netw.* **13**, 411–430 (2000). https://doi.org/10.1016/S0893-6080(00)00026-5

[13] Grodecki, K. *et al.* Enhanced Raman spectra of hydrogen-intercalated quasi-free-standing monolayer graphene on 4H-SiC(0001). *Physica E* **117**, 113746 (2020). https://doi.org/10.1016/j.physe.2019.113746

[14] Grodecki, K. & Murawski, K. New data analysis method for time-resolved infrared photoluminescence spectroscopy. *Appl. Spectrosc.* **75**, 596-599 (2020). https://doi.org/10.1177/0003702820969700

[15] Hong-Yan, L., Zhao, Q. H., Ren, G. L. & Xiao, B. J. Speech enhancement algorithm based on independent component analysis. in *5th Int. Conf. on Natural Computation (ICNC 2009)* **2**, 598–602 (2009). https://doi.org/10.1109/ICNC.2009.76

[16] Wen, S. & Ding, D. FASTICA-based firefighters speech noise reduction. in *Proc. 2015 of 8th Int. Congress on Image and Signal Processing (CISP 2015)* 1423–1426 (2016). https://doi.org/10.1109/CISP.2015.7408106

[17] Yue, F. Y. *et al.* Optical characterization of defects in narrow-gap HgCdTe for infrared detector applications. *Chin. Phys. B* **28**, 17104–017104 (2019). https://doi.org/10.1088/1674-1056/28/1/017104

[18] Zhang, X. *et al.* Infrared photoluminescence of arsenic-doped HgCdTe in a wide temperature range of up to 290 K. *J. Appl. Phys.* **110**, 043503 (2011). https://doi.org/10.1063/1.3622588